



# Photo-enhanced activity of Pt and Pt–Ru catalysts towards the electro-oxidation of methanol



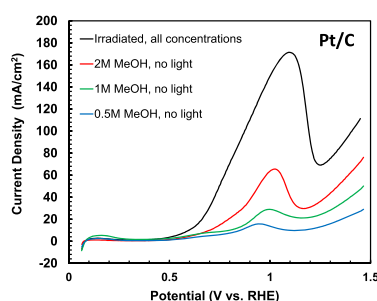
Dheevesh V. Arulmani, Jennie I. Eastcott, Stephanie G. Mavilla, E. Bradley Easton\*

Faculty of Science, University of Ontario Institute of Technology, 2000 Simcoe Street North, Oshawa, Ontario, Canada L1H 7K4

## HIGHLIGHTS

- Pt/C has enhanced methanol oxidation activity when irradiated with visible light.
- Pt–Ru/C show enhanced methanol oxidation activity when irradiated with visible light.
- Photo-enhancement occurs in both the presence and absence of TiO<sub>2</sub>.
- Photo-enhancement is greater with light in the near-UV region than with near-IR.
- Both catalysts show no photo-enhancement towards formic acid oxidation.

## GRAPHICAL ABSTRACT



## ARTICLE INFO

### Article history:

Received 13 July 2013

Received in revised form

30 August 2013

Accepted 31 August 2013

Available online 20 September 2013

### Keywords:

Methanol oxidation reaction

Photoelectrooxidation

Platinum

Platinum–Ruthenium

Titanium dioxide

Direct methanol fuel cell

## ABSTRACT

Electrocatalyst materials, consisting of Pt or Pt–Ru supported on carbon with and without TiO<sub>2</sub>, are evaluated for their activity towards the methanol oxidation reaction (MOR) in 1.0 M H<sub>2</sub>SO<sub>4</sub> at 25 °C in the presence and absence of visible light irradiation. Electrochemical studies showed that enhanced MOR activity is achieved upon irradiation with visible light for each catalyst, in both the presence and absence of TiO<sub>2</sub>. Irradiation leads to no improvement in activity towards the formic acid oxidation reaction (FAOR) indicating that irradiation aids in the removal of adsorbed intermediate species, such as CO, during MOR. While the presence of a TiO<sub>2</sub> support does lead to an increase in activity upon irradiation, about 50% of the improvements arise solely from the irradiation of the metal-containing electrocatalysts themselves.

© 2013 Elsevier B.V. All rights reserved.

## 1. Introduction

Direct methanol fuel cells (DMFCs) exhibit feasibility as an environmentally sustainable power source for an assortment of stationary, mobile, and transportation applications. As a

subdivision of polymer electrolyte membrane fuel cells, DMFCs demonstrate advantages associated with high energy densities, portability, low operating temperatures, and the simplicity of handling a liquid fuel [1–5]. The electrochemical advantages of standard hydrogen-based fuel cells are significantly offset by the inefficiencies of hydrogen production, storage, and dispensing [6]. However, the use of liquid methanol as a liquid carrier of hydrogen in DMFCs has been suggested as methanol has substantially higher storage and production capacities, and distribution of liquid fuel

\* Corresponding author. Tel.: +1 905 721 8668x2936; fax 1 905 721 3304.

E-mail address: [Brad.Easton@uoit.ca](mailto:Brad.Easton@uoit.ca) (E.B. Easton).

could be achieved through adapting current infrastructure [1,7]. The high energy density of methanol fuel makes DMFCs more attractive than conventional hydrogen-fuelled cells for portable applications [1,8]. Nonetheless, intrinsic power density outputs of DMFCs are constrained by the complexity of the reactions and must be enhanced to facilitate commercialization. Slow reaction kinetics and contamination at the cathode from methanol crossover currently limit the application of this technology [1,9]. Consequently, a combination of theoretical and technological breakthroughs will unravel the path to a feasible DMFC system.

The ideal cell voltage of 1.21 V for DMFCs is presently unattainable. This is a result of overpotential losses at both the anode and the cathode. While the overpotential losses for the oxygen reduction reaction (ORR) at a Pt cathode are significant, the losses are greater at the anode due to the slower kinetics of the methanol oxidation reaction (MOR). Thus, improving MOR activity is the most prominent method to enhance intrinsic power densities of DMFCs [4,10].

The substantially low kinetics and the high activation energy at the anode can be attributed to the complexity of the stages and the numerous steps and paths by which the MOR is facilitated, which is depicted in Fig. 1 [9,10]. The complexity of the MOR results in reduced DMFC performance [4]. Furthermore, intermediate species such as carbon monoxide can bind strongly to the Pt surface, blocking active sites and slowing the overall reaction greatly [4]. Alloy catalysts, namely Pt–M alloys, have been employed to reduce the incidence of CO poisoning [11]. The presence of the second metal can allow the oxidation of CO at lower potentials than with Pt [11]. Pt–M alloys can consist of a variety of metals including M = Ru, Os, Sn, Mn, Ti, Cr, Fe, Co, Ni [11,12], Pt–Ru in particular has been shown to be especially successful in prevention of Pt catalyst poisoning [12,13]. Another prevalent issue with DMFCs is methanol crossover as fuel diffuses through the polymer electrolyte membrane. In addition to fuel waste, this also results in a mixed cathode potential that further reduces DMFC performance [4]. These energetically unfavorable processes and the complexity of the MOR lead to a high activation energy that substantially minimizes fuel cell voltage and decreases system lifetime [5].

The investigation of photosensitive catalysts has been at a forefront for the improvement of multiple applications including pollutant degradation [14], wastewater remediation [15], and hydrogen production [16]. Titanium dioxide ( $\text{TiO}_2$ ) is highly active towards many photocatalytic reactions and therefore is widely used and well-studied [17]. Titania photocatalysts are also corrosion resistant in acidic environments, operate at low operational temperatures, and are low cost materials [18]. However,  $\text{TiO}_2$  catalysts are only active in the UV region ( $\lambda < 400 \text{ nm}$ ), which reduces their efficacy for some applications. Addition of a noble metal such as platinum can serve as a co-catalyst to suppress recombination of electron-hole pairs and enhance photocatalytic activity in both the UV and visible regions [19]. The use of platinum, a traditional catalyst for fuel cells, with  $\text{TiO}_2$  suggests that such photocatalysts could be used in fuel cell electrodes.

The use of  $\text{TiO}_2$  in fuel cell electrode development as a substrate for catalyst deposition has been reported [20–23]. However, their

contribution to the catalytic process has only recently been studied. Previous reports have demonstrated that the electrooxidation of methanol can be enhanced when  $\text{TiO}_2$  is combined with Pt/C catalysts exposed to UV irradiation [8,19,24,25]. This research focuses on the study of the individual electrode components, namely the electrocatalyst (Pt/C and Pt–Ru) and  $\text{TiO}_2$ , and their photo-enhancement of the MOR in the presence and absence of light in the near-ultraviolet to infrared region. In addition, catalysts were tested for photo-activity towards formic acid oxidation in order to gain mechanistic insights.

## 2. Experimental

### 2.1. Electrode preparation

The catalysts studied were 20 wt% Pt on Vulcan XC72 or 40 wt% Pt–Ru (1:1 atomic ratio) on Vulcan XC72 (E-TEK BASF, Somerset, NJ), hereafter referred to as Pt/C and Pt–Ru/C. Samples for electrochemical measurements were prepared as electrocatalyst layers immobilized on glassy carbon electrodes prepared from inks. Catalyst inks were prepared by dispersing catalyst material in a 50:50 mixture of isopropyl alcohol and water (400  $\mu\text{L}$ ) followed by 100  $\mu\text{L}$  of 5% Nafion<sup>®</sup> (DuPont<sup>™</sup> de Nemours, Wilmington, DE) solution. For electrodes prepared with  $\text{TiO}_2$  anatase (Evonik Degussa P25 powder, Parsippany, NJ), the  $\text{TiO}_2$  (20  $\mu\text{m}$  average particle size) was initially ground with a mortar and pestle and mixed with the original catalyst material. A 1:1 ratio of  $\text{TiO}_2$  and catalyst was used for this work. The inks were sonicated for approximately 60 min to achieve a uniform suspension. 5  $\mu\text{L}$  of ink were deposited onto a polished 5 mm diameter glassy carbon (GC) disk electrode (Pine Research Instruments, Durham, NC) and allowed to dry for at least 30 min. Total (metal) catalyst loadings were calculated to be between  $0.15 \pm 0.02 \text{ mg cm}^{-2}$ .

### 2.2. Electrochemical measurements

All electrochemical experiments were performed in a jacketed 3-electrode cell using a saturated calomel reference electrode (SCE) and a platinum wire counter electrode. Electrochemical measurements were made using Pine Instruments AFCBP1 bipotentiostat controlled using Aftermath software (Pine Research Instruments, Durham, NC). All data reported here have been corrected to the reversible hydrogen electrode (RHE) potential. The electrolyte consisted of  $\text{N}_2$ -purged 1 M  $\text{H}_2\text{SO}_4$  and either MeOH or formic acid. Electrocatalytic activity was measured in the presence and absence of a light source. The light source used for irradiation was a 10,500 lumen halogen lamp that emits a light intensity of  $300 \text{ mW cm}^{-2}$ . The lamp was set up 12.5 cm from the electrode surface at an angle of incidence of  $0^\circ$  for a constant photon flux. Specific additive dichroic filters, infrared IR-A/IR-B longpass filters and multi-layer dielectric UV filters (Edmund Optics, Barrington, NJ) facilitated transmittance of  $\sim 70$ – $90\%$  within the wavelengths and frequencies of 200–700 nm, 390–490 nm, 490–580 nm, 580–730 nm, and 700–2250 nm. In order to ensure that the light source did not heat the cell, temperature was maintained at  $25 \pm 1^\circ\text{C}$  by flowing cold water through the jacket and monitored with a thermometer. Measurements were made in the absence of the light filters unless specified.

## 3. Results and discussion

### 3.1. Catalyst characterization

Enhancements in MOR or formic acid oxidation activity with photo-electro-oxidation (upon irradiation) were evaluated based on the magnitude of the oxidation current and also the onset

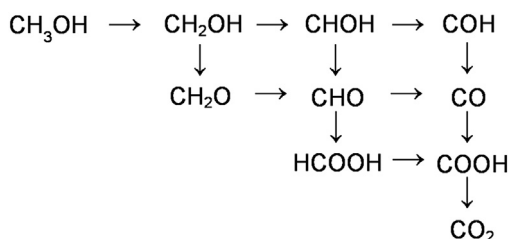


Fig. 1. Reaction network for methanol oxidation reaction [4].

**Table 1**  
Summary of MOR activity of each catalyst in the presence and absence of irradiation. ECSA was measured in 1 M H<sub>2</sub>SO<sub>4</sub> at 25 °C. All other measurements were made in 1 M H<sub>2</sub>SO<sub>4</sub> containing 1 M CH<sub>3</sub>OH at 25 °C.

Sample	Scan rate	ECSA in 1 M H <sub>2</sub> SO <sub>4</sub> (m <sup>2</sup> g <sub>Pt</sub> <sup>-1</sup> )	MOR current peak (mA cm <sup>-2</sup> )	Enhancement with irradiation (+%)	Onset potential (mV)	Δ onset potential with irradiation (mV)
Pt	20 mV s <sup>-1</sup>	45	20	495%	816	–155
Pt irradiated		43	119		661	
Pt TiO <sub>2</sub>		21	31	297%	1040	–342
Pt TiO <sub>2</sub> irradiated		22	123		698	
Pt–Ru	10 mV s <sup>-1</sup>	–	8	500%	592	–141
Pt–Ru irradiated		–	48		451	
Pt–Ru TiO <sub>2</sub>		–	10	420%	651	–215
Pt–Ru TiO <sub>2</sub> irradiated		–	52		436	

potential for the oxidation process, which we have defined as the potential corresponding to 5% of the peak faradaic current [26,27], which are compiled in Table 1 for each catalyst layer tested.

### 3.2. Pt/C catalysts

#### 3.2.1. MOR activity

Fig. 2(a) displays the MOR activity achieved using Pt/C in the presence and absence of irradiation. The presence of irradiation has a profound enhancement of the MOR, with a 5-fold enhancement of the peak oxidation current. Similarly, the onset potential is substantially reduced by more than 150 mV. This type of enhancement for Pt/C in the absence of TiO<sub>2</sub> was not observed by Li et al. [8]. The most likely reason for this is the difference light sources; Li et al. employed a UV irradiation source whereas we have used a broader spectrum near-UV to infrared light source.

The MOR activity with Pt/C + TiO<sub>2</sub> also shows photo-enhancement, with a 3-fold increase in current and a reduced

onset potential. However, the presence of TiO<sub>2</sub> does not lead to substantial improvement over the photo-electrochemical activity of Pt/C itself. A likely reason for this is that the addition of TiO<sub>2</sub> into the catalyst layer will somewhat reduce the electrochemically active surface area (ECSA) of accessible Pt, and therefore reduce the maximum performance of the electrode. This is supported by the data in Fig. 3, which shows the CVs obtained in the absence of methanol for both Pt/C and Pt/C + TiO<sub>2</sub>, that were used to determine ECSA. The addition of TiO<sub>2</sub> into the catalyst layer reduces the ECSA value to ca. half the ECSA achieved in its absence (21 m<sup>2</sup> g<sup>-1</sup> compared to 44 m<sup>2</sup> g<sup>-1</sup>, see Table 1). Thus, the presence of TiO<sub>2</sub> may be blocking otherwise active catalytic sites. When the MOR activity is corrected for the difference in available surface area, we do observe about a 2-fold increase in activity when TiO<sub>2</sub> is present, as shown in Fig. 4. Thus, if improvements can be made in the dispersion of TiO<sub>2</sub> into the catalyst layer so that Pt utilization remains high, then greater raw performance could be achieved.

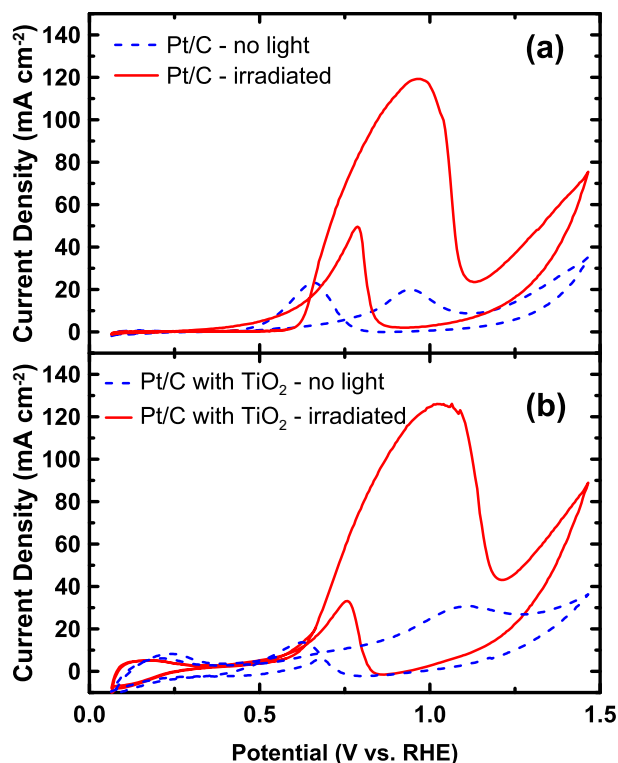


**Fig. 2.** Cyclic voltammograms (CVs) obtained for (a) Pt/C and (b) Pt/C with TiO<sub>2</sub> in the presence and absence of irradiation. Measurements were made at a sweep rate of 20 mV s<sup>-1</sup> in 1 M H<sub>2</sub>SO<sub>4</sub> containing 1 M CH<sub>3</sub>OH at 25 °C.

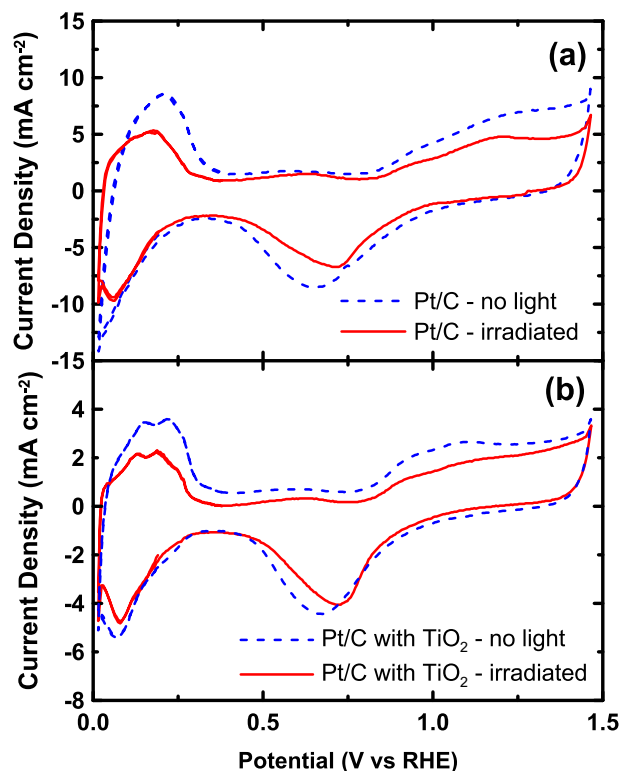


**Fig. 3.** CVs obtained for (a) Pt/C and (b) Pt/C with TiO<sub>2</sub> in the presence and absence of irradiation. Measurements were made at a sweep rate of 100 mV s<sup>-1</sup> in 1 M H<sub>2</sub>SO<sub>4</sub>.

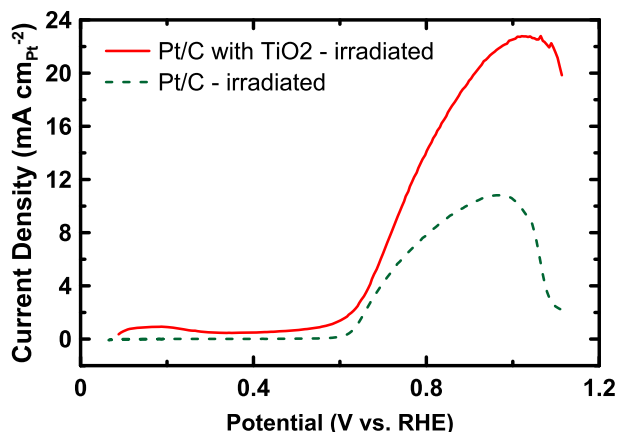


**Fig. 4.** Comparison of the photo-enhanced methanol oxidation activity obtained for Pt/C and Pt/C with TiO<sub>2</sub>. Current has been corrected to the available surface area of Pt determined from the CVs shown in Fig. 3. Measurements were made at a sweep rate of 20 mV s<sup>-1</sup> in 1 M H<sub>2</sub>SO<sub>4</sub> containing 1 M CH<sub>3</sub>OH at 25 °C.

The mechanism of methanol photo-catalytic oxidation in the presence of TiO<sub>2</sub> is not well understood, but it has been generally proposed that photo-irradiation by UV light generates electron holes at TiO<sub>2</sub>, which subsequently react with methanol species to generate CO<sub>2</sub> [24,28,29]. This photocurrent would be collected in addition to any current from an electrochemical pathway. This mechanism will not occur for catalysts composed solely of Pt/C since there are no semi-conductors present. Thus, the reason for photo-enhancement in the absence of TiO<sub>2</sub> must be due to a change in the kinetics in the electrochemical mechanism at the catalyst surface. For MOR, the removal of adsorbed CO is considered the rate determining step, thus we propose that the mechanism of photo-enhanced activity of Pt/C must be due to an improvement in the removal of CO intermediates.

To study this further, CVs were obtained in the absence of methanol for both Pt/C and Pt/C + TiO<sub>2</sub> with and without photo-irradiation, which are shown in Fig. 3. The presence of irradiation does have a clear impact on the CV features, and were essentially the same in both the presence and absence of TiO<sub>2</sub>. The high potential Pt oxide formation/stripping waves appear to be suppressed when the sample is irradiated. At intermediate potentials there is also a noticeable decrease in the double layer capacitance current (near 0.42 V vs. RHE). There is also a noticeable change in the H<sub>desorption</sub> features upon irradiation, with these features appearing at slightly lower potentials. However, integration of the H<sub>desorption</sub> peaks reveal only a 12% decrease in charge under those waves. Surprisingly, there is little change in the H<sub>adsorption</sub> waves upon irradiation, that when integrated to determine charge produce near identical ECSA values (see Table 1). Based on these CVs we can infer that there is indeed a change in the energetics at the Pt surface upon photo-irradiation.

The activity of the irradiation sensitive Pt/C catalyst was evaluated with methanol concentrations of 0.5 M, 1 M, and 2 M, as shown in Fig. 5. The oxidation current densities (at ~1.1 V) increase proportionately with the methanol concentration when no irradiation is employed. Irradiation led to larger currents though the magnitude of the oxidation current and onset potential was unaffected by methanol concentration. This indicates that after a threshold concentration of methanol, the rate of photo-electro-oxidation is finite. Based on this assertion, DMFC performance enhancements can be achieved without using high concentrations of MeOH. This could also lead to additional performance gains since lower concentrations of methanol in the anode feed would mean

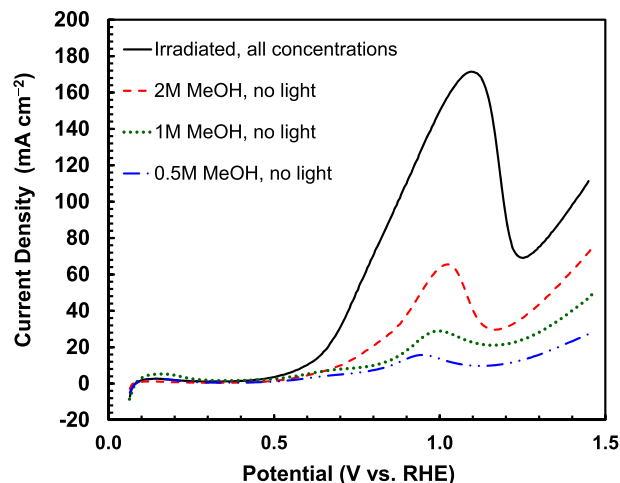


**Fig. 5.** LSVs obtained for Pt/C in the presence and absence of irradiation using different concentrations of MeOH. Measurements were made at 25 °C using a sweep rate of 20 mV s<sup>-1</sup> in 1 M H<sub>2</sub>SO<sub>4</sub> at 25 °C.

reduced methanol crossover and therefore enhanced cathode performance [10].

### 3.2.2. Formic acid oxidation activity

In order to better understand how irradiation influences the MOR mechanism on Pt/C, the photo-electro-oxidation of formic acid with Pt/C was also studied. Fig. 6 compares the activity of Pt/C towards the formic acid oxidation reaction (FAOR) in the presence and absence of irradiation. No gains in performance were achieved, rather a slight decline in performance was observed, consistent with the slight decline in ECSA observed upon irradiation. Since irradiation has no impact on the kinetics of FAOR, this implies that the photo-activity towards MOR must be due to the improved kinetics for steps that involve the creation or consumption of surface –OH groups on the Pt surface, which would aid in the removal of adsorbed CO groups during the MOR. While the CVs obtained in the absence of methanol do not show an increase in Pt–OH activation at lower potentials, there is a clear change in the energetics related to surface species formation and this must aid in the removal of adsorbed CO species. Future work will focus on more detailed mechanistic studies of this process.

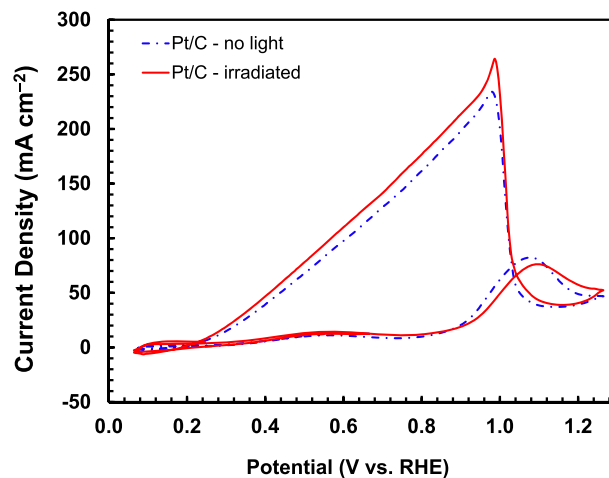


**Fig. 6.** Formic acid oxidation activity obtained for Pt/C in the presence and absence of irradiation. Measurements were made in 1 M H<sub>2</sub>SO<sub>4</sub> containing 1 M HCOOH at 25 °C at a sweep rate of 100 mV s<sup>-1</sup>.

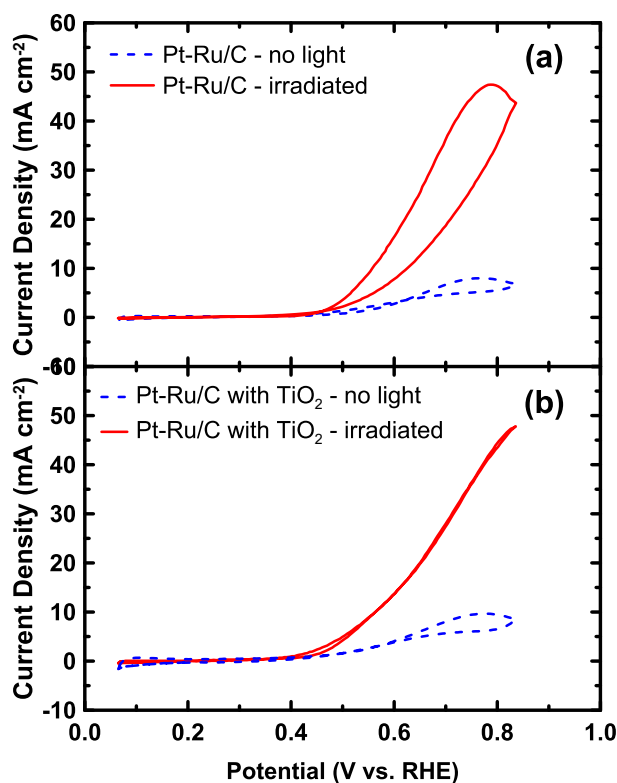


Fig. 7. CVs obtained for (a) Pt–Ru/C and (b) Pt–Ru/C with TiO<sub>2</sub> in the presence and absence of irradiation. Measurements were made at a sweep rate of 10 mV s<sup>−1</sup> in 1 M H<sub>2</sub>SO<sub>4</sub> containing 1 M CH<sub>3</sub>OH at 25 °C.

### 3.3. Pt–Ru/C catalysts

#### 3.3.1. MOR activity

Pt–Ru is the best known catalyst for the MOR. Also, the presence of Ru may change the photosensitivity of the catalysts and therefore its photo-electrochemical performance. To study this, the MOR activity of catalysts layers comprising of Pt–Ru/C and Pt–Ru/C + TiO<sub>2</sub> were evaluated in the presence and absence of irradiation which is shown in Fig. 7. As expected, the Pt–Ru has a lower onset potential for than Pt/C catalysts in all cases. Like the Pt/C catalyst, the Pt–Ru catalyst displayed a photocatalytic enhancement in the absence of TiO<sub>2</sub>, with a peak current that is ca. five times larger compared to the non-irradiated case. Similarly, the presence of TiO<sub>2</sub> did shift the onset potential for MOR to lower values but did not result in larger currents being produced. However, the presence of TiO<sub>2</sub> no doubt decreases the ECSA compared to the Pt–Ru/C catalyst. Determination of a true ECSA value for alloy catalysts like Pt–Ru is non-trivial and was not attempted from CVs in the absence of methanol (not shown). Nonetheless, it is safe to assume that the ECSA will drop in the presence of TiO<sub>2</sub> by about the same factor (50%) as that measured with Pt/C. Thus, we can still infer that the addition of TiO<sub>2</sub> is having a positive effect on MOR activity on a catalyst area-specific basis (Fig. 8).

#### 3.3.2. Irradiation energy

In order to understand the impact of irradiation energy of photo-enhancement of MOR activity, a series of spectroscopic filters were inserted between the light source and the electrochemical cell. Fig. 8 shows that MOR activity of Pt–Ru + TiO<sub>2</sub> increases as the section of the visible light spectrum that is transmitted shifts from the higher wavelengths (near-infrared region) to lower wavelengths (near-ultraviolet region). A similar relationship

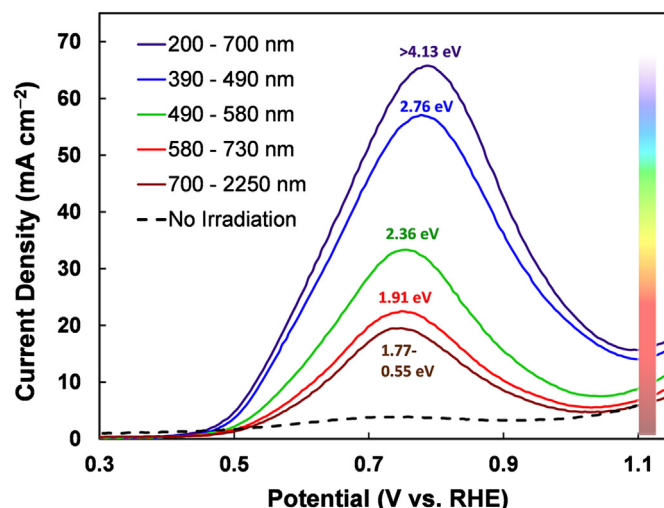


Fig. 8. LSVs obtained for Pt–Ru/C with TiO<sub>2</sub> using different light filters. Measurements were made in 1 M H<sub>2</sub>SO<sub>4</sub> containing 1 M CH<sub>3</sub>OH at 25 °C.

was present with subtractive dichroic filters, where DMFC performance increased relative to the irradiation energy levels in the exposed bandwidth.

## 4. Conclusions

Electrochemical measurements demonstrate that using different combinations of TiO<sub>2</sub> with both Pt/C and Pt–Ru/C lead to photo-sensitive catalyst layers that can be used for MOR when irradiated with visible light. Considerable photo-enhancement (up to 5-fold) was achieved using just the metal supported catalysts themselves. Since Pt/C showed no photo-enhancement towards the FAOR, it is inferred that irradiation facilitated the removal of absorbed MOR intermediate species such as CO. While the addition of TiO<sub>2</sub> to the catalyst layer does show benefits in terms of area-specific photo-activity, its presence in the catalyst layer reduces the ECSA leading to a reduction in electrocatalytic MOR current so that performance is no better than photo-irradiating the metal catalysts themselves. By filtering the irradiated light it was demonstrated that MOR activity is higher when irradiation sources employed light shifted towards the near-UV region.

## Acknowledgements

This work was supported by the Natural Sciences and Engineering Research Council of Canada (NSERC) through the Discovery Grants program and UOIT. JE acknowledges scholarship support from NSERC and the Ontario Graduate Scholarship (OGS) program. SM acknowledges scholarship support from the OGS program.

## References

- [1] K.G. Nishanth, P. Sridhar, S. Pitchumani, A.K. Shukla, J. Electrochem. Soc. 158 (2011) B871–B876.
- [2] G. Selvarani, S. Maheswari, P. Sridhar, S. Pitchumani, A.K. Shukla, J. Electrochem. Soc. 156 (2009) B1354–B1360.
- [3] A. Arico, P. Creti, E. Modica, G. Monforte, V. Baglio, V. Antonucci, Electrochim. Acta 45 (2000) 4319–4328.
- [4] A.M. Zainoodin, S.K. Kamarudin, W.R.W. Daud, Int. J. Hydrogen Energy 35 (2010) 4606–4621.
- [5] N.W. Deluca, Y.A. Elabd, J. Polym. Sci. Pt. B-Polym. Phys. 44 (2006) 2201–2225.
- [6] K. Adamson, P. Pearson, J. Power Sources 86 (2000) 548–555.
- [7] G. Cacciola, V. Antonucci, S. Freni, J. Power Sources 100 (2001) 67–79.
- [8] W. Li, Y. Bai, F. Li, C. Liu, K. Chan, X. Feng, X. Lu, J. Mater. Chem. 22 (2012) 4025–4031.



- [9] S. Arisetty, U. Krewer, S.G. Advani, A.K. Prasad, J. Electrochem. Soc. 157 (2010) B1443–B1455.
- [10] J. Larminie, A. Dicks. (2003).
- [11] H. Liu, C. Song, L. Zhang, J. Zhang, H. Wang, D. Wilkinson, J. Power Sources 155 (2006) 95–110.
- [12] E. Antolini, Mater. Chem. Phys. 78 (2003) 563–573.
- [13] A.S. Arico, S. Srinivasan, V. Antonucci, Fuel Cells 1 (2001) 133–161.
- [14] S. Yamazaki, Y. Fujiwara, S. Yabuno, K. Adachi, K. Honda, Appl. Catal. B-Environ. 121 (2012) 148–153.
- [15] S.S. Thind, G. Wu, A. Chen, Appl. Catal. B-Environ. 111 (2012) 38–45.
- [16] R.P. Antony, T. Mathews, C. Ramesh, N. Murugesan, A. Dasgupta, S. Dhara, S. Dash, A.K. Tyagi, Int. J. Hydrogen Energy 37 (2012) 8268–8276.
- [17] B. Ohtani, O.O. Prieto-Mahaney, D. Li, R. Abe, J. Photochem. Photobiol. A. 216 (2010) 179–182.
- [18] K. Koci, K. Mateju, L. Obalova, S. Krejčíková, Z. Lacný, D. Placha, L. Capek, A. Hospodková, O. Solcova, Appl. Catal. B-Environ. 96 (2010) 239–244.
- [19] X. Li, Z. Zhuang, W. Li, H. Pan, Appl. Catal. A-Gen. 429 (2012) 31–38.
- [20] P. Xiao, X. Guo, D. Guo, H. Song, J. Sun, Z. Lv, Y. Liu, X. Qiu, W. Zhu, L. Chen, U. Stimming, Electrochim. Acta 58 (2011) 541–550.
- [21] S. Chen, M. Malig, M. Tian, A. Chen, J. Phys. Chem. C 116 (2012) 3298–3304.
- [22] Q. Lv, M. Yin, X. Zhao, C. Li, C. Liu, W. Xing, J. Power Sources 218 (2012) 93–99.
- [23] K. Hirakawa, M. Inoue, T. Abe, Electrochim. Acta 55 (2010) 5874–5880.
- [24] K. Park, S. Han, J. Lee, Electrochem. Commun. 9 (2007) 1578–1581.
- [25] Y. Guo, J. He, S. Wu, T. Wang, G. Li, Y. Hu, H. Xue, X. Sun, J. Tang, M. Liu, J. Power Sources 208 (2012) 58–66.
- [26] L. Birry, J.H. Zagal, J. Dodelet, Electrochem. Commun. 12 (2010) 628–631.
- [27] A.D. Pauric, B.J. MacLean, E.B. Easton, J. Electrochem. Soc. 158 (2011) B331–B336.
- [28] A.S. Polo, M.C. Santos, R.F.B. de Souza, W.A. Alves, J. Power Sources 196 (2011) 872–876.
- [29] K. Drew, G. Girishkumar, K. Vinodgopal, P. Kamat, J. Phys. Chem. B 109 (2005) 11851–11857.